

Influence of spin-orbit scattering on the Ruderman-Kittel-Kasuya-Yosida effect in superconducting thin films

J. E. Tkaczyk* and P. M. Tedrow

Francis Bitter National Magnet Laboratory, Massachusetts Institute of Technology, Cambridge, Massachusetts 02139

(Received 18 February 1992)

Spin-polarized tunneling was used to study exchange effects as a function of spin-orbit scattering rate at the surface of thin Al films, each covered with a submonolayer of Gd. The spin-orbit scattering rate was controlled by the deposition of a Pt layer on the side of the Al film opposite that covered with Gd. At sufficient Pt coverages, the Zeeman splitting of the conduction electrons is washed out, but the magnitude of the polarization is unchanged. Furthermore, polarization of the same magnitude is observed in both the superconducting and normal state. These results are understood in terms of the dependence of the conduction-electron spin susceptibility on the spin-orbit scattering rate.

INTRODUCTION

It is well known that the exchange interaction between the spin of an impurity and those of the conduction electrons of a normal metal gives rise to a spin polarization of the conduction electrons, and that this polarization mediates the coupling between impurity spins. However, this Ruderman-Kittel-Kasuya-Yosida¹ (RKKY) spin polarization is suppressed in the BCS superconductors due to singlet pairing. The spin polarization $P(r)$ is related to the susceptibility $\chi(q)$, where q is the wave vector:

$$P(r) = \int dr' \chi(r-r') B_{\text{ex}}(r') = \sum_q \chi(q) B_{\text{ex}}(q) e^{iq \cdot r},$$

where B_{ex} represents the exchange field. The RKKY spin polarization is derived by substituting the free-electron expression for $\chi(q)$. The sharp cutoff at the Fermi wave number gives rise to a polarization with spatial extent on the scale of the Fermi wavelength λ_F . The important difference between the superconducting and normal states is that the long-range part of the spin susceptibility is significantly depressed in the superconductor.² This fact has been verified in Knight shift experiments on Al, but only after a series of conflicting experimental results.³ More recently, the absence of the RKKY effect in superconductors with low spin-orbit scattering has been demonstrated by spin-polarized tunneling experiments.⁴ Tunneling measurements provide an unambiguous means of investigating such systems, as the tunneling conductance is closely related to the density of states.⁵

The spin susceptibility of a superconductor with spin-orbit scattering has been worked out by Kaufman and Entin-Wohlman.⁶ With the introduction of spin-orbit scattering on the order of the superconducting energy gap, $\hbar/\tau_{\text{so}} \sim 3\Delta$, the spin susceptibility of the superconductor can be of the order of that in the normal state.² One then expects the presence of the RKKY polarization in response to a local exchange potential. This possibility is examined here through the controlled introduction of spin-orbit scattering using thin-film deposition techniques. Spin-orbit scattering is introduced by the deposi-

tion of a surface layer of Pt onto a thin Al film. Spin-polarized tunneling is used to compare the RKKY polarization in the weak and strong spin-orbit cases and in the superconducting and normal states.

EXPERIMENT

Three types of multilayer structures are the objects of this study. Each was fabricated by vacuum deposition onto liquid-nitrogen-cooled glass substrates. The first structure is an Al/Pt bilayer consisting of a 4.0-nm-thick Al film covered with two monolayers of Pt. Tedrow and Meservy have experimentally demonstrated the effect of Pt on the critical field⁷ and the density of states⁸ of thin Al films. For each monolayer of Pt, the spin-orbit scattering rate \hbar/τ_{so} was found to increase by 3.2 meV. This scattering rate is large in the sense that in order to resolve the Zeeman splitting $2\mu B$ in the presence of this scattering rate, the field B must be of the order $\sim 3.2 \text{ meV}/2\mu_B = 27.6 \text{ T}$, while in pure Al, $B \sim 1 \text{ T}$ is sufficient.

The second structure consists of a Gd/Al bilayer constructed from a 4.0-nm-thick Al film covered with a submonolayer of Gd ($\sim 3 \text{ atoms/nm}^2$). Previous measurements have established three easily distinguishable features which appear in the superconducting density of states as consequences of the exchange interaction from the Gd.⁴ The first-order perturbative effect is a splitting of the electron energy like that produced by a magnetic field (i.e., Zeeman splitting). This first-order effect results in a sizable energy splitting of the tunneling conductance, as first demonstrated in the experiments of Tedrow, Tkaczyk, and Kumar.⁹ In second order, exchange scattering of electrons decreases the transition temperature T_c , and broadens the density of states, producing a broadened conductance curve and smaller gap.¹⁰ The third consequence of the exchange interaction, the one of interest in this paper, is the RKKY spin polarization of the conduction electrons. This appears in the tunneling conductance as a characteristic asymmetry with respect to zero-bias voltage.

Finally, the two perturbations to the aluminum film (i.e., exchange and spin-orbit scattering) were combined

in a third structure consisting of a Gd/Al/Pt trilayer. The Pt and Gd thicknesses were nominally the same as those in the first two structures. In fact, the first and third structures were made at the same time except for a shutter operation during Gd deposition. For each of these three structures, a standard procedure was used to construct a tunnel junction on the side of the Al film covered with Gd and/or opposite the side with the Pt layer. This junction provides access to the density of states at this surface. A second Al film formed the counter electrode of these junctions. Conductance measurements were performed in a ^3He cryostat at a temperature $T=0.45$ K.

RESULTS

The conductance of an Al-Al₂O₃-Al/Pt junction in an applied magnetic field of $B=2.12$ T is shown in Fig. 1. This field is chosen so that both electrodes, the Al film and Al/Pt bilayer, are superconducting. The peak that is typically observed at the sum of the energy gaps (sum-gap peak) is here split into two peaks. The energy separation was measured and found to equal the Zeeman splitting of the Al film for the applied field, i.e., $2\mu B=0.25$ meV.

In Fig. 2 the conductance of an Al-Al₂O₃-Gd/Al junction is shown for two values of the applied field. In curve *a*, the applied field is below the critical field of both the Al and Gd/Al electrodes. Again, the sum-gap peak in the conductance is split by the difference $2\mu B_{\text{ex}}$ in the Zeeman splitting of the electrons in the top and bottom electrodes. No asymmetry with respect to zero-bias voltage is observed, indicating the lack of a RKKY spin polarization. The curve *b* was taken in an applied field above the critical field of the Gd/Al electrode. The Al electrode remains superconducting and the spin states are Zeeman split by the applied magnetic field $2\mu B=0.43$ meV. The conductance is asymmetric, indicating polarization of the Gd/Al electrode in the normal state.

The conductance for a junction of the form Al-Al₂O₃-Gd/Al/Pt is shown in Fig. 3 in an applied field

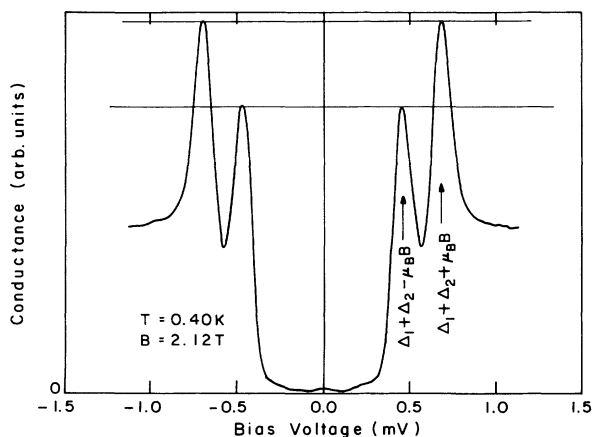


FIG. 1. The conductance of an Al-Al₂O₃-Al/Pt junction, where two monolayers of Pt mix the spin state of the electrons in the Al/Pt electrode. The voltage splitting of the sum-of-the-gaps peak corresponds to the Zeeman splitting of the electrons in the Al electrode, $2\mu B=0.25$ meV.

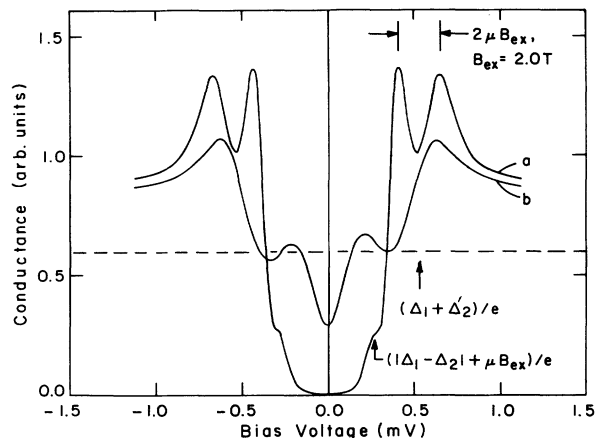


FIG. 2. The conductance of the Al-Al₂O₃-Gd/Al junction measured for two values of the applied magnetic field: *a*, $B=0.17$ T; *b*, $B=3.72$ T.

$B=3.34$ T, where the Gd/Al/Pt electrode is normal. Features similar to that seen in Fig. 2(b) are evident. Figure 4 shows the conductance of the same junction in an applied field of $B=2.12$ T, where both electrodes are superconducting. This is the same field used in Fig. 1 for the control junction with no Gd. The energy splitting of the sum-gap peak is the same as that measured from Fig. 1, $\Delta E=0.25$ meV. In contrast to the *S-I-S* tunneling curves of Figs. 1 and 2(a), a characteristic asymmetry with respect to zero-bias voltage is evident. The peak at -0.6 meV is seen to be higher than that at $+0.6$ meV, while the peak at $+0.4$ meV is higher than the peak at -0.4 meV.

DISCUSSION

Spin-polarized tunneling

Measurements of the superconducting tunneling conductance presented in Figs. 1–4 are understood in terms

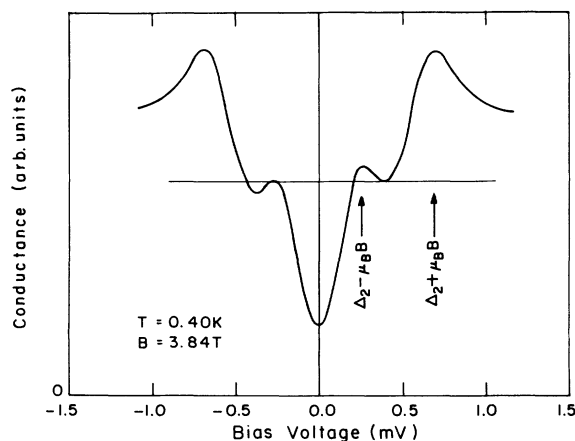


FIG. 3. The conductance of an Al-Al₂O₃-Gd/Al/Pt junction measured in a magnetic field where only the Al electrode is superconducting. The asymmetry with respect to zero bias is associated with a spin polarization of electrons in the Gd/Al/Pt electrode.

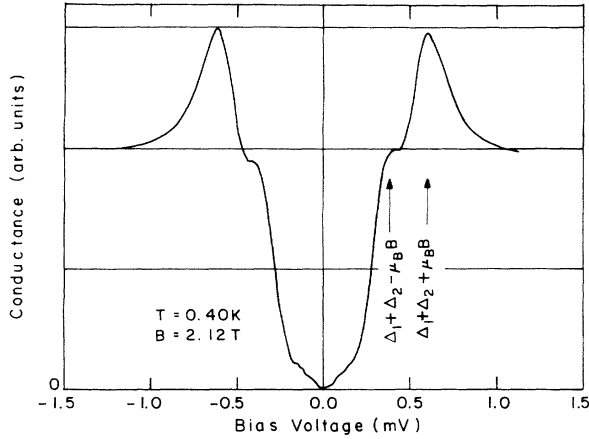


FIG. 4. The conductance of the same junction used in Fig. 3 but at a lower magnetic field for which both electrodes are superconducting. The asymmetry indicates a spin polarization of the electrons in the Gd/Al/Pt electrode. The conductance of the corresponding control junction (i.e., no Gd) is shown in Fig. 1.

of the semiconductor model,¹¹ which is schematically represented in Fig. 5. A wealth of information is available as long as one of the electrodes is superconducting. The number of conductance peaks, their voltage position, and relative heights give information about the spin-dependent densities of states of the junction electrodes. In all cases above, a superconducting Al counterelectrode was used, as its behavior is well documented and the native oxide forms a good tunneling barrier. The superconducting Al counterelectrode serves as a probe of the density of states even when the multilayer structures are in the normal state.

Two established rules must be considered in the interpretation of the spin-polarized tunneling conductance.⁵ First, in addition to tunneling at constant energy, the quasiparticles do not flip their spins during tunneling through an Al_2O_3 barrier.¹² Secondly, a superconducting thin film with small spin-orbit scattering has its density of states split into spin-up and spin-down parts by a magnet field.¹³ The left-hand side of Fig. 5 presents the density of states of the two electrodes of the tunnel junction for various conditions. The shaded area represent the filled states, while the clear areas are empty states. The bias voltage moves one density of states with respect to the other. Tunneling can occur only when a filled state on one side of the barrier is opposite an empty state at the same energy on the other side of the barrier. The right-hand side of the figure shows the resulting conductance as a function of voltage.

Figure 5(a) illustrates the case of *S-I-S* tunneling in a magnetic field when the two superconducting electrodes have low spin-orbit scattering. The resulting conductance is unchanged from that in zero field. Because of conservation of spin, tunneling across the barrier is forbidden until the applied bias voltage shifts the density of states an energy equal to the sum of the energy gaps.

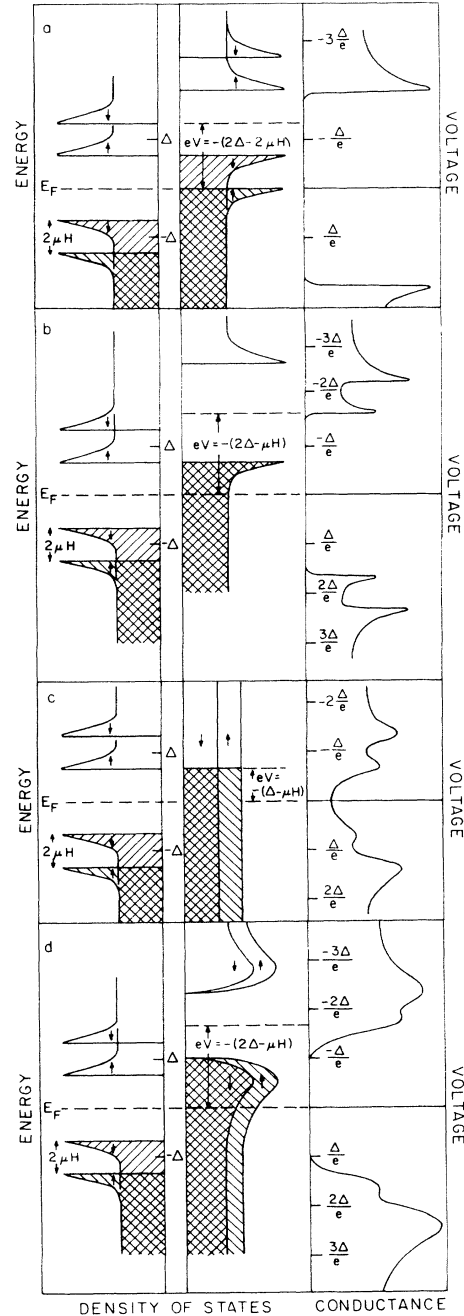


FIG. 5. Schematic representation (semiconductor model) of the tunneling process connecting the density of state to the measured conductance. In all cases, the counterelectrode (left side) represents the density of states of a superconductor with low spin-orbit scattering in a magnetic field. The superconducting density of states is split by the Zeeman energy. Curve *a* represents the case of the right electrode of this same type. In curve *b*, the density of states of the right electrode is not spin split. In curve *c*, the right electrode is a ferromagnet. Curve *d* represents speculation as to the case of a superconductor with spin polarization, which is possible in the case of strong spin-orbit scattering combined with a RKKY interaction.

Figure 5(b) illustrates the extreme case where the Zeeman splitting of the electrons in one electrode vanishes because of spin-orbit scattering. The sum-gap peak in the conductance is split by the Zeeman energy. This serves as a model of conductance data presented in Fig. 1.

The general case of S_1 - I - S_2 tunneling where the energy gaps and Zeeman splitting is different for the two electrodes is similarly modeled. The result is that the sum-gap peak is split symmetrically about its zero-field position. The splitting of the peak is equal to the difference in Zeeman splitting of the two electrodes. Possible reasons for differences in Zeeman energy include spin-orbit scattering (discussed above), Fermi-liquid effects,¹⁴ and the first-order effect of the exchange interaction.⁴ The last effect accounts for the splitting of the sum-gap peaks observed in the conductance data presented in Fig. 2(a). A second feature of S_1 - I - S_2 tunneling is that at high temperatures, additional peaks appear at the difference of the energy gaps. These peaks are small in magnitude and result due to a thermally activated population of quasiparticle states above the gap. One of the difference peaks is observed in the conductance data presented in Fig. 2(a). This corresponds to the more heavily populated peak in the density of states.

The effects discussed up to this point result in structure in the tunneling conductance that is symmetric with respect to zero-bias voltage. The origin of asymmetry is illustrated in Fig. 5(c). Spin polarization of the conduction electrons at the Fermi level of a ferromagnet causes the inner conductance peak at $V = -(\Delta - \mu H)/e$ to be higher than the one at $V = (\Delta - \mu H)/e$, while the outer peaks at $V = \pm(\Delta + \mu H)/e$ have the opposite asymmetry of magnitude. Experiments using $4f$ and $3d$ band ferromagnets as one electrode of the tunnel junction have implied that the degree of asymmetry of the conductance is proportional to the spin polarization of the itinerant electrons at the surface of the ferromagnet.¹⁵ A value for the polarization $P = (n_{\uparrow} - n_{\downarrow})/(n_{\uparrow} + n_{\downarrow})$ can be calculated from the conductance peak heights.¹⁶

The representation in Fig. 5(c) is taken to explain the conductance data presented in Fig. 2(b). The conductance is asymmetric indicating polarization of the Gd/Al electrode in the normal state. A $2.9 \pm 0.6\%$ polarization was calculated using the four peak heights. This is the expected order of magnitude, considering that the polarization observed in Gd metal is 13% and the sample has $\sim \frac{1}{3}$ atomic layer coverage of Gd. Note that the asymmetry is a large effect in comparison to other features routinely measured by tunneling; for instance, those due to phonons.

Spin-orbit scattering and the RKKY effect

The conductance data for the Gd/Al/Pt trilayer are presented in Figs. 3 and 4 and these results represent the main finding of this paper. In an applied field sufficient to drive the Gd/Al/Pt trilayer normal (Fig. 3), the Zeeman splitting of the Al electrode is observed. In addition,

an asymmetry corresponding to a polarization $P = 4.1 \pm 0.6\%$ can be associated with the Gd/Al/Pt electrode. This is of the same order as that obtained in the low spin-orbit scattering case from Fig. 2(b) for a Gd/Al electrode.

It may appear contradictory that the introduction of sufficient spin-orbit scattering to wash out the Zeeman splitting in the superconducting density of states does not reduce the spin polarization in the normal state. However, the Pauli principle restricts spin-orbit scattering to states within $k_B T$ of the Fermi level. Only those states at the Fermi surface are spin mixed. The states involved in the localized RKKY effect are generally far from the Fermi surface. As a result, to a first approximation the RKKY spin polarization of the conduction electrons in the normal state is expected to be unaffected by spin-orbit scattering. A related discussion is given by Ferrell in the analogous case of the Knight shift.¹⁷

Measurements presented in Fig. 4 are made at a lower applied field for which the Gd/Al/Pt electrode is superconducting. Splitting of the sumgap peaks is observed and is of the same magnitude $2\mu H$ as that in Fig. 2(a). In addition, the curves are asymmetric, indicating a spin polarization of the itinerant electrons in the superconducting Gd/Al/Pt electrode. A polarization $P = 3.3 \pm 0.6\%$ of the same magnitude as that in the normal state was determined from the peak height ratios. One may note that the structure in Fig. 4 is less sharp than the S - I - S conductance curves in Figs. 1 and 2(a). This is believed to be a consequence of depairing effects associated with the exchange interaction¹⁰ and the combination of spin-orbit scattering and a magnetic field.¹² In Fig. 5(d), we speculate as to the shape of the density of states of a superconductor with a spin polarization and depairing, which is possible in the case of strong-spin-orbit scattering.

SUMMARY

Spin-polarized tunneling has been used to study the polarization of the conduction electrons produced by Gd atoms on the surface of thin Al films. In the low spin-orbit scattering case, the polarization vanishes in the superconducting state, as expected from the calculated behavior of the spin susceptibility. The addition of strong spin-orbit scattering from a Pt surface layer allows the polarization to persist in the superconducting state.

ACKNOWLEDGMENTS

We would like to thank R. MacNabb for fabrication of the tunnel junctions. This work was supported by the National Science Foundation Grant No. DMR-8618072. The Francis Bitter National Magnet Laboratory is supported at the Massachusetts Institute of Technology by the National Science Foundation. J. E. Tkaczyk was supported by Department of Energy Contract No. DE-FG02-84ER45094.

*Present address: General Electric Research and Development, Schenectady, N.Y.

- ¹M. A. Ruderman and C. Kittel, Phys. Rev. **96**, 99 (1954); T. Kasuya, Prog. Theor. Phys. Jpn. **16**, 45 (1956); K. Yosida, Phys. Rev. **106**, 893 (1957).
- ²P. Fulde and J. Keller, in *Superconductivity in Ternary Compounds II*, edited by Ø. Fischer and M. B. Maple (Springer-Verlag, New York, 1982).
- ³R. H. Hammond and G. M. Kelly, Phys. Rev. Lett. **18**, 156 (1967); H. L. Fine, M. Lipsicas, and M. Strongin, Phys. Lett. **29**, 366 (1969).
- ⁴J. E. Tkaczyk and P. M. Tedrow, Phys. Rev. Lett. **61**, 1253 (1988).
- ⁵P. Fulde, Adv. Phys. **22**, 667 (1973).
- ⁶M. Kaufman and O. Entin-Wohlman, Physica B **84**, 77 (1976).
- ⁷P. M. Tedrow and R. Meservey, Phys. Rev. Lett. **43**, 384 (1979).
- ⁸P. M. Tedrow and R. Meservey, Phys. Rev. B **25**, 171 (1982).
- ⁹P. M. Tedrow, J. E. Tkaczyk, and A. Kumar, Phys. Rev. Lett. **56**, 1746 (1986).
- ¹⁰A. A. Abrikosov and L. P. Gor'kov, Zh. Eksp. Teor. Fiz. **39**, 1781 (1961) [Sov. Phys.—JETP **12**, 1243 (1961)]; M. A. Woolf and F. Reif, Phys. Rev. **137**, A557 (1965).
- ¹¹J. Bardeen, Phys. Rev. Lett. **6**, 57 (1961); M. Tinkham, *Introduction To Superconductivity* (Krieger, Huntington, NY, 1980), p. 44.
- ¹²R. Meservey, P. M. Tedrow, and R. C. Bruno, Phys. Rev. B **11**, 4224 (1975).
- ¹³R. Meservey, P. M. Tedrow, and P. Fulde, Phys. Rev. Lett. **25**, 1270 (1970).
- ¹⁴P. M. Tedrow, J. T. Kucera, D. Rainer, and T. P. Orlando, Phys. Rev. Lett. **52**, 1637 (1984); J. A. X. Alexander, T. P. Orlando, D. Rainer, and P. M. Tedrow, Phys. Rev. B **31**, 5811 (1985).
- ¹⁵R. Meservey, D. Paraskevopoulos, and P. M. Tedrow, Phys. Rev. B **22**, 1331 (1980); Phys. Rev. Lett. **37**, 856 (1976).
- ¹⁶P. M. Tedrow and R. Meservey, Phys. Rev. B **7**, 318 (1973).
- ¹⁷R. A. Ferrell, Phys. Rev. Lett. **3**, 262 (1959).